coatings

MDPI

Article

Production of Phosphorescent Coatings on 6082 Aluminum Using $Sr_{0.95}Eu_{0.02}Dy_{0.03}Al_2O_{4-\delta}$ Powder and Plasma Electrolytic Oxidation

Krisjanis Auzins [1], Aleksejs Zolotarjovs [1], Ivita Bite [1], Katrina Laganovska [1], Virginija Vitola [1], Krisjanis Smits [1,*] and Donats Millers [1,2]

1 Institute of Solid State Physics, University of Latvia, Kengaraga str. 8, LV-1063 Riga, Latvia; krisjanis.auzins@gmail.com (K.A.); aleksejs.zol@gmail.com (A.Z.); ivita.bite@gmail.com (I.B.); katrina.laganovska@gmail.com (K.L.); virgiinija@gmail.com (V.V.); dmillers@latnet.lv (D.M.)

2 ElGoo Tech Ltd., Peldu str. 7, LV-3002 Jelgava, Latvia

* Correspondence: smits@cfi.lu.lv; Tel.: +371-26-538-386

Received: 28 October 2019; Accepted: 11 December 2019; Published: 16 December 2019

Abstract: In this study, a new approach for producing phosphorescent aluminum coatings was studied. Using the plasma electrolytic oxidation (PEO) process, a porous oxide coating was produced on the Al6082 aluminum alloy substrate. Afterwards, activated strontium aluminate ($SrAl_2O_4$: Eu^{2+}, Dy^{3+}) powder was filled into the cavities and pores of the PEO coating, which resulted in a surface that exhibits long-lasting luminescence. The structural and optical properties were studied using XRD, SEM, and photoluminescence measurements. It was found that the treatment time affects the morphology of the coating, which influences the amount of strontium aluminate powder that can be incorporated into the coating and the resulting afterglow intensity.

Keywords: plasma electrolytic oxidation (PEO); aluminum 6082; luminescent coatings; phosphorescence

1. Introduction

Persistent luminophores or "phosphors" are materials that exhibit long-lasting luminescence that is often called phosphorescence, and these have been known and widely used for more than a century in various glow-in-the-dark objects. During the 20th century, the most commonly used persistent luminophore was zinc sulfide (ZnS) in combination with a suitable activator ion (e.g., copper, cobalt) [1]. However due to the comparatively low intensity and duration of persistent luminescence, the use of this persistent luminophore has decreased in favor of strontium aluminate-based persistent luminophores. Discovered in the mid-20th century, strontium aluminate [2] activated with divalent europium ($SrAl_2O_4$: Eu^{2+}) has since become one of the most widely used persistent luminophores. With the addition of Dy^{3+} in the matrix in the 1990s [3], the afterglow time increased significantly without the use of any radioactive materials. Compared to ZnS-persistent luminophores, it has superior luminescence intensity, and its afterglow duration can reach up to 20 h [4]. There are various methods for synthesizing strontium aluminates (commonly in the form of powder), the most popular being the solid-state method [5], combustion synthesis [6], the sol–gel method [7], and the precipitation method [8].

Long-lasting luminescence materials mostly find applications in places where lighting is necessary in case of a power failure such as emergency exit aisles in buildings or public transportation vehicles. Safety signs, road markings [9], and parts of glow-in-the-dark objects such as watch arms, remote control buttons, toys, and other everyday items are another domain in which long persistent luminescence

materials are used. At the moment, most of the persistent luminescence objects are created by applying phosphorescent paint to the desired objects, which a lot of the time includes metallic surfaces, e.g., safety signs. With time, the phosphorescent paint can start to wear off and lose its brightness; thus, a more durable method for applying luminescent coatings to different surfaces should be developed.

Plasma electrolytic oxidation (PEO), also known as micro-arc oxidation (MAO), is one of the newest and most studied methods for treating valve metal surfaces, which creates a porous ceramic oxide layer on the metal surface and is most commonly used on metals such as Mg [10], Al [11], Ti [12], and Zr [13]. These metals naturally develop only a thin oxide layer of a few nanometers, which does not protect the surface of the metal from mechanical damage; so, it is necessary to create an additional protective layer. Although PEO phenomena have been known for around 100 years, more rigorous research on this method was begun in the late 1990s by Yerokhin [14]. While similar to conventional anodization, the main difference of PEO is the use of high voltages, which are usually above 400 V. During the beginning phases of treatment, a dielectric oxide layer is grown, and at some point, dielectric breakdown occurs. This leads to local high-energy spark discharges through the dielectric layer. These discharges cause small channels to form on the coating, which results in the increased porosity of the coating [15]. The morphology and properties of the PEO coating can be modified by changing the voltage and current density as well as the polarity and pulse duration [16].

Metal alloys such as aluminum or magnesium are widely used in automotive [17], aerospace [18], and aviation industries because of their light weight and ease of workability. Despite being mostly used for enhancing the wear and corrosion resistance properties of metals [19,20], the PEO method has proven to be useful for creating functionalized coatings, and in the last few years, there has been a growing amount of research devoted to studying these prospects. PEO has been used for producing photocatalytic [21], gas sensing [22], and dosimetric [23] coatings as well as coatings for biomedical applications such as dental [24] and orthopedic implants [25]. One of the more recent fields of study has been PEO application for the development of luminescent coatings. Several articles report the successful incorporation of rare earth luminescent ions in the coatings of different metals [26,27].

One of the latest innovations is the development of long-lasting luminescence coatings using the PEO process. The combination of the protective properties of a PEO coating and long-lasting luminescence opens up possibilities for different practical applications. By adding raw materials in powder form to the electrolyte, it was possible to synthesize strontium aluminate luminophore on an aluminum substrate in a single-step PEO process [28]. However, the method has a few disadvantages that need to be addressed. Large amounts of lanthanide oxides need to be mixed in the electrolyte in order to produce a coating with long afterglow, which significantly increases costs. Another problem is the aging or degradation of the electrolytes, which leads to a decreased quality of the coating, as it affects the characteristics of discharges and the porosity of the PEO coating [29]. Lastly, the quantum yield of such coatings compared to commercially available activated strontium aluminate powder is still relatively low. Although the method of developing long-lasting luminescence coatings is very promising for various practical applications, the shortcomings of it must be overcome, and different approaches should be studied.

In this article, a new method of filling the cavities of PEO coatings with commercially available activated strontium aluminate powder to produce phosphorescent aluminum oxide coatings is developed and studied. Such a method would decrease the amount of raw material consumption and possibly increase the luminescence quantum yield of long-lasting luminescence coatings.

2. Materials and Methods

2.1. Materials

Commercial aluminum alloy Al6082 was used as a substrate material (Al: 95.2%–98.3%; Cr: 0.25% max; Cu: 0.1% max; Fe: 0.5% max; Mg: 0.6 to 1.2%; Mn: 0.4% to 1.0%; Si: 0.7%–1.3%; Ti: 0.1% max; Zn: 0.2% max; residuals: 0.15% max). The aluminum was cut using a mechanical cutting blade to

form specimens in 60 mm × 15 mm × 3 mm sizes with a total area of 22.5 cm^2. The electrolytes consisted of 600 mL of deionized water (conductivity 0.0555 μSm/cm) and 1.0 g/l KOH ("RK Chem"). Commercial Sigma Aldrich strontium aluminate powder doped with europium, and dysprosium ions ($Sr_{0.95}Eu_{0.02}Dy_{0.03}Al_2O_4$, purity ≥ 99%) were used for pore-filling purposes.

2.2. Synthesis

For the production of the PEO coatings, a custom-built power supply unit BS4000 (A5V1000/300) by Elgoo Tech Ltd (Jelgava, Latvia) was used. The power output of the unit is up to 5 kW with a voltage limit at 1000 V and a current limit at 5 A. The unit is controlled via a computer interface to set up the desired voltage and current parameters. All the samples were prepared using a non-pulsed direct current with 700 V and 3 A limiting parameters. The surface area covered during PEO treatment was 16.65 cm^2, which yielded a current density of 0.18 A/cm^2. Before the PEO process, aluminum substrates were washed with deionized water and acetone. The container for the PEO process is made of double-walled glass with inlets for water cooling. To ensure sufficient cooling, the electrolyte was constantly stirred using a magnetic stirrer. During the PEO process, large amounts of heat are dissipated, and a part of the electrolyte evaporates. To keep the amount of electrolyte unchanged, constant refilling is necessary. After the PEO process, samples were washed with deionized water and dried in air at room temperature. Afterwards, approximately 0.1 g of commercial activated strontium aluminate powder was mixed with ethanol and milled in an agate mortar with a pestle for 5 min. Then, the mixture was applied to PEO coatings using a pipette and using the tip of the pipette equally distributed along the surface of the sample. Then, the sample was put in a furnace at 80 °C for 5 min to evaporate the ethanol. When the powder had dried, the sample was laid on a firm surface, and another similarly sized non-treated aluminum sheet was carefully placed on top of it, and constant pressure (approx. 1 kg/cm^2) was applied to the system for 5 min to ensure that the powder was pressed into the pores. Afterwards, the sample was washed thoroughly with deionized water to flush away any particles that did not adhere well enough to the surface. In total, 11 PEO samples were synthesized using different treatment durations and studied during this research. The parameters for all samples are shown in Table 1. A graphical step-by-step process representation is shown in Figure 1.

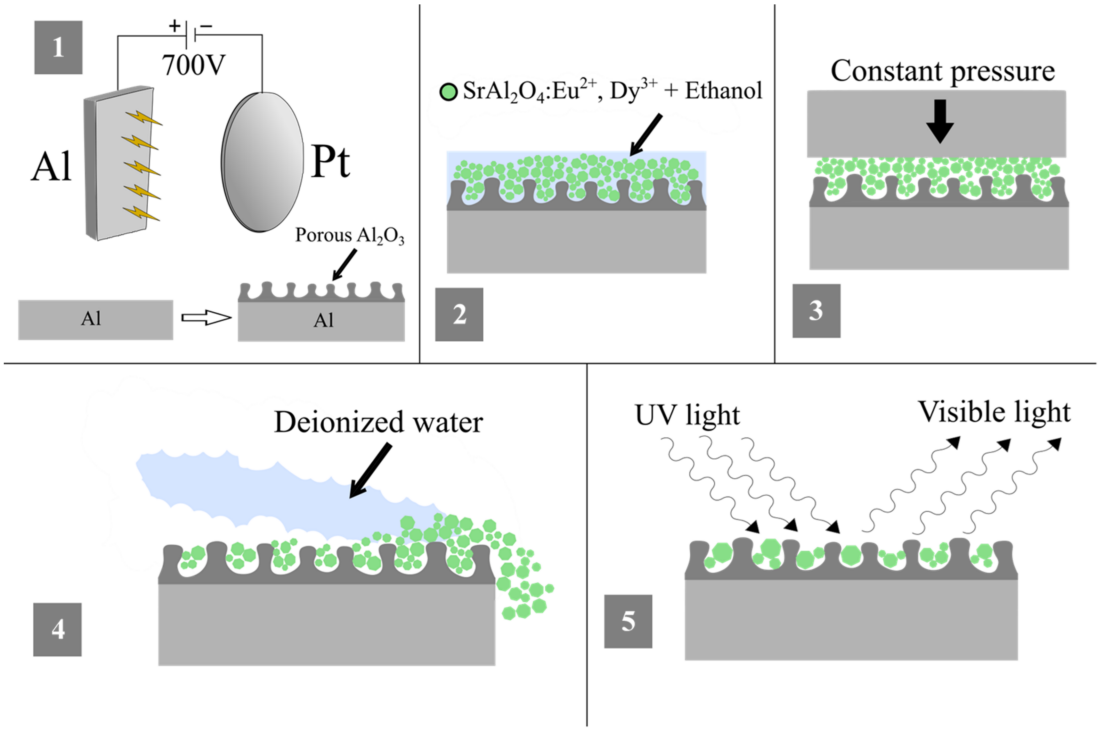

Figure 1. Graphical step-by-step process representation.

Table 1. Plasma electrolytic oxidation (PEO) sample synthesis parameters.

Sample No.	Voltage, V	Current Density, A/cm^2	Duration, Min	Powder Filling
P15N	700	0.18	15	No
P20N			20	
P30N			30	
P40N			40	
P45N			4560	
P60N				
P15Y	700	0.18	15	Yes
P20Y			20	
P30Y			30	
P40Y			40	
P45Y			45	
P60Y			60	

2.3. Analysis Methods

Sample morphology and phase composition were studied using scanning electron microscopy (SEM) and X-ray diffraction (XRD). SEM images were taken using a Phenom-World Phenom Pro scanning electron microscope registering backscattered electron (BSE) images with 10 kV acceleration voltage. Cross-section images were taken using an SEM Tescan Lyra equipped with an energy dispersive X-ray spectrometer (EDX) operated at 15 kV. X-ray diffraction patterns were acquired using a Rigaku MiniFlex 600 X-ray diffractometer using a cathode voltage of 40 kV and current of 15 mA with Cu Kα radiation (1.5418 Å). The step size for the XRD measurements was 0.05 2θ with a scan speed of 10 2θ/min. Photoluminescence (PL) spectra measurements were made using an Andor Shamrock B 303i spectrograph in combination with an Andor DU-401A-BV CCD camera. The excitation source for PL measurements was a CryLas Nd:YAG laser (266 nm) (spot size on sample: approximately 3 mm in diameter). Luminescence decay kinetics were measured using a Horiba iHR320 monochromator coupled with a Hamamatsu R928P photomultiplier tube using a 5 mW 405 nm diode laser as the excitation source.

3. Results and Discussion

The pore-filling method developed and used during this study allows the production of long afterglow phosphorescent PEO coatings. The naming of this method may be debated, since the powder is filled in the cavities or cracks of the PEO coating rather than pores, but the idea of filling up empty space in the coating remains. The produced samples can be seen in Figure 2. Visually, the appearance of the coating does not differ before and after filling the pores. During normal conditions, the coating is light gray and does not exhibit any luminescence properties. When the sample is illuminated by UV light, the electrons from Eu^{2+} are transferred to the traps, and after ceasing the excitation, the electrons from traps recombine with Eu^{3+} [30,31], and the sample exhibits a bright green long afterglow visible with the naked eye, which is characteristic to the $SrAl_2O_4$: Eu^{2+}, Dy^{3+} luminophore. The phosphorescent coating has good adhesion to the aluminum alloy surface as it was obtained during electrochemical oxidation, and it is also to some extent water-resistant, although strontium aluminate is partly soluble in water, and the luminescent coating might degrade over time without additional protection.

3.1. Structure and Morphology

The XRD patterns of the acquired PEO coatings before and after pore filling are shown in Figure 3. The samples mainly contain γ-Al_2O_3 phase alumina and small traces of α-Al_2O_3 phase. Al peaks from the substrate are also visible in the pattern. The sample after pore filling additionally contains peaks that correspond to $SrAl_2O_4$. The detected phases in all the samples are presented in Table 2. While

the γ-Al_2O_3 phase can be detected in all the samples, the α-Al_2O_3 is only visible in samples with a treatment duration longer than 30 min, although some samples that exceed the 30-min duration still do not show an α-Al_2O_3 phase. This is due to the presence of an α-Al_2O_3 phase in a small quantity, and therefore, it is right on the detection limit of the XRD device. The $SrAl_2O_4$ phase is detected only in samples with longer PEO durations, i.e., 40 and 45-min treatments. This is because the longer treatment time allows more powder to be filled into the coating, which can be explained by analyzing SEM images. Although samples P15Y, P20Y, and P30Y have the luminescent powder in them (as confirmed by luminescence measurements later), the content is not enough to be detected by XRD.

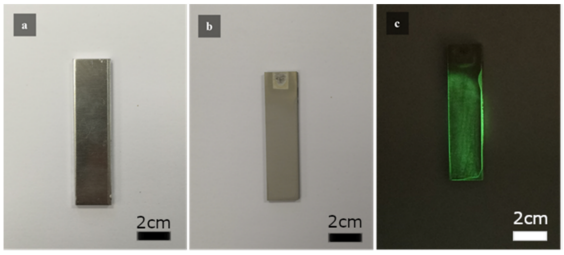

Figure 2. Sample (**a**) before PEO (P45N), (**b**) after PEO and pore filling (P45Y), and (**c**) after excitation with UV light.

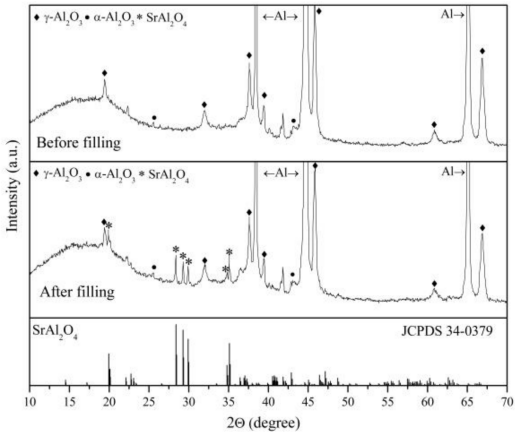

Figure 3. XRD patterns of 45-min sample before and after pore filling.

Table 2. Detected phases by XRD analysis in samples.

Sample Name	γ-Al_2O_3	α-Al_2O_3	$SrAl_2O_4$
P15N	X	-	-
P20N	X	-	-
P30N	X	-	-
P40N	X	X	-
P45N	X	X	-
P60N	X	X	-
P15Y	X	-	-
P20Y	X	-	-
P30Y	X	X	-
P40Y	X	X	X
P45Y	X	X	X
P60Y	X	X	-

The SEM images displaying morphology of the coatings after different PEO treatment times are shown in Figure 4. It can be seen that longer PEO treatment duration develops thicker and more densely packed cavities and pores. After 15 and 20 min (Figure 4a,b), the pores are very small with a size of around 1 micrometer. After 30 min or a longer time of treatment (Figure 4c–e), the pores and cavities are larger (2–10 micrometers) and denser.

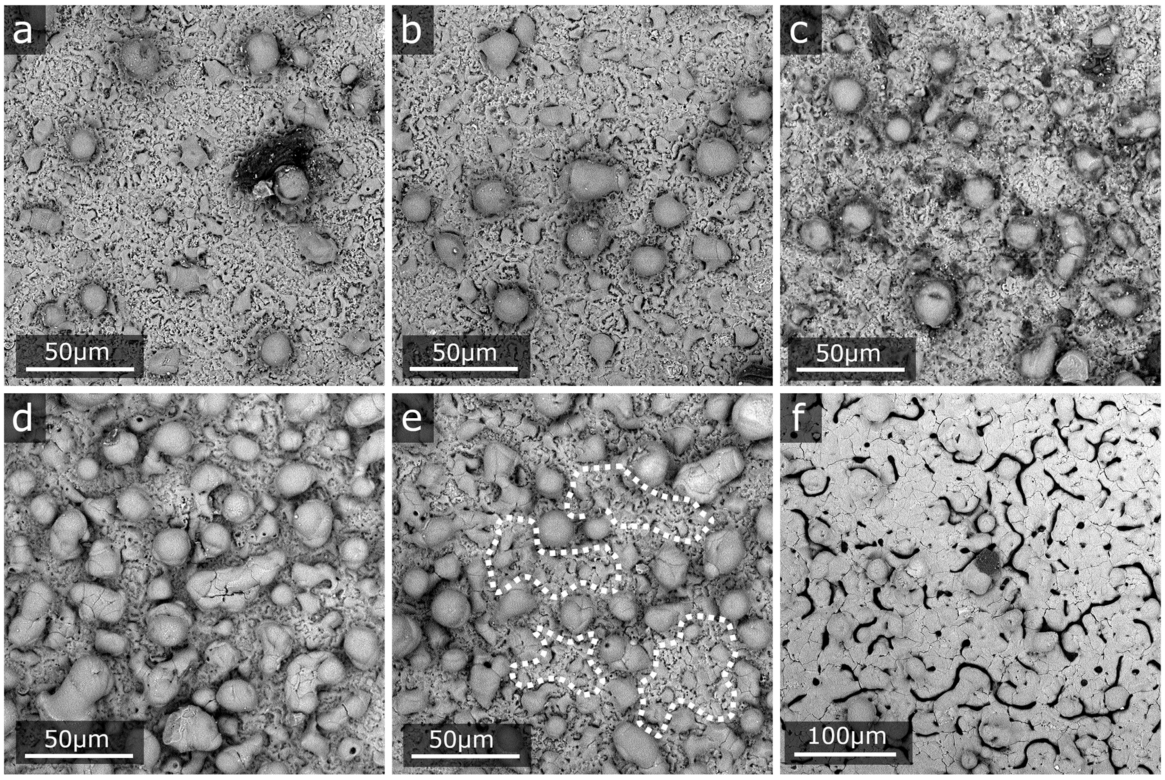

Figure 4. SEM images of samples before pore filling (**a**) 15 min – P15N; (**b**) 20 min – P20N; (**c**) 30 min – P30N; (**d**) 40 min – P40N; (**e**) 45 min – P45N (cavities are marked with dashed line), and (**f**) 60 min – P60N.

The optimal PEO time was found to be 45 min, as continuing the treatment longer leads to the transition of the coating to a different, less porous structure. The effect is shown in Figure 4f for P60N. Beginning from the sides of the sample, the plasma discharges and gradually becomes less dense, and the morphology transforms to one without large pores and containing thin long cavities. After approximately 60 min, most of the sample morphology had transformed (P60N). This was found to reduce the amount of powder that can be filled into the coating significantly. Figure 5a displays commercial strontium aluminate powder. It can be seen that the average grain size is around 30–50 micrometers. To facilitate the incorporation of powder into the coating, milling was necessary. Figure 5b shows strontium aluminate powder after milling for 5 min. The majority of grains after milling are smaller than 10 micrometers. Sieving was not performed after the milling. SEM images with powder filled into the coating are shown in Figure 5c. The particles build into the cavities that are formed from round alumina structures. In Figure 5d, the surface is shown at a smaller magnification, which represents how densely the powder has filled up the pores of the sample with 45-min PEO treatment.

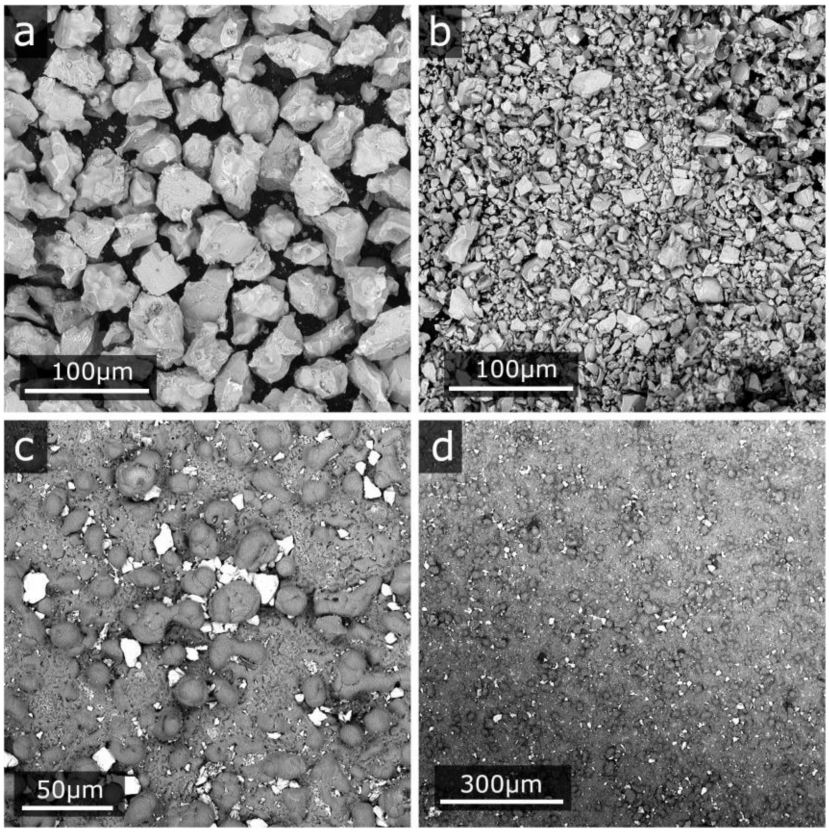

Figure 5. (**a**,**b**) Strontium aluminate powder before and after milling; (**c**,**d**) P45Y sample after pore filling

To analyze the incorporation of powder in the pores and evaluate the thickness of the coating, a cross-section image of the P45Y sample was taken (Figure 6). As one can see, the thickness of the coating varies greatly due to the high porosity of the alumina, and the average thickness is measured at approximately 40 µm. Moreover, evaluation of the composition of the coating gives a confirmation of the presence of strontium aluminate powder in the pores. An interesting observation can be made: the Mg atoms are also detected in both the aluminum alloy (Mg is the main alloying element in Al6082 alloy) and in the coating (taken from the alloy itself and incorporated in the structure of the alumina). Other elements are below the detection limit of the setup.

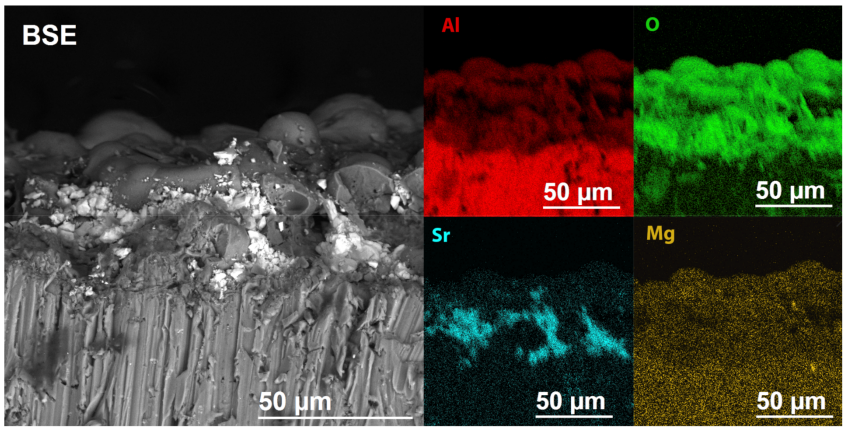

Figure 6. Cross-section BSE SEM image of the coating with element mapping for Al, O, Sr, and Mg.

3.2. Luminescence

To compare and study the optical properties of different samples, photoluminescence measurements were carried out in identical conditions for all the samples. To ensure that luminescence properties do not change after milling, the powder PL measurements were carried out for both powders. The PL spectra of the sample after pore filling were compared to powder samples and are displayed in Figure 7. All intensities have been normalized. Strontium aluminate powder before and after milling shows no significant difference in PL spectra, which means that the structure of the grains has not been disrupted; however, the absolute intensity decreased by 31%. The PEO sample with the 45-min treatment time after pore filling also exhibits the characteristic strontium aluminate luminescence band with a maximum at 530 nm. The additional peak can be seen at 693 nm; this includes the characteristic R1 and R2 lines of Cr^{3+} ion luminescence in an α-Al_2O_3 matrix (ruby). The intensity of this luminescence band correlates with the α-phase content, which in turn is related to the PEO processing time. The ion itself is acquired from the substrate, aluminium alloy, has the Cr as an additive in it. An increase in intensity in the near-IR region for the PEO sample is a second order of the UV part; the blue alumina luminescence is usually present in PEO coatings.

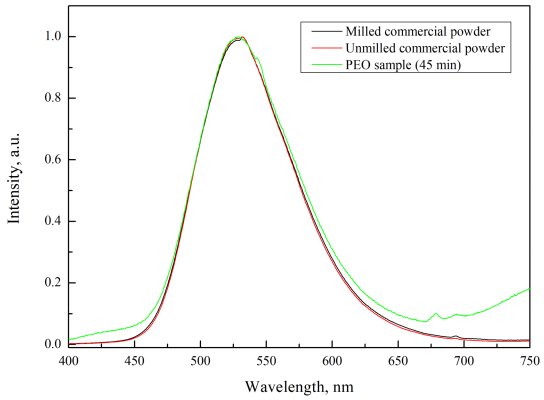

Figure 7. Photoluminescence spectra of powder before and after milling and 45-min PEO sample (P45Y).

In Figure 8, the PL spectra of samples with different PEO treatment times after pore filling are shown. The shape of the luminescence bands does not change except for the intensity of luminescence maximum. It can be seen that a longer PEO treatment duration leads to higher PL intensity, which is displayed in the insert of Figure 8. The PL intensity is directly related to the amount of strontium aluminate powder that can be incorporated into the pores and cavities of the coating. Samples with 15 and 20-min treatment time show almost identical PL intensity, while increasing the PEO processing time further increases the amount of powder that can be incorporated in the coating; a steady growth of luminescence is observed until 45 min of processing time (sample P45Y). One would expect that increasing the PEO treatment duration even further would lead to an increase in PL intensity; however, that is not the case. An even longer treatment time leads to the opposite effect, where the luminescence intensity drops significantly. This can be explained by the morphology of the coating; all the samples with a processing time longer than 45 min exhibit a transformation of the surface to a denser packed, less porous structure (can be seen earlier in SEM Figure 4f). The dense coating without cavities prevents the strontium aluminate powder adhering to the surface; there are no features for particles to attach to. To compensate for that, one can use smaller particles and fill the pores still present in a coating (e.g., black spots in Figure 4f); however, not only the overall intensity of the powder will decrease with the size of the particles, but the amount of powder that is possible to incorporate will decrease as well. This leads to the conclusion that 45 min at given PEO parameters is the optimal time for the chosen application. The 60-min sample (P60Y) is not presented in Figure 8 due to the low intensity of the signal, as no luminescent powder is present in the pores.

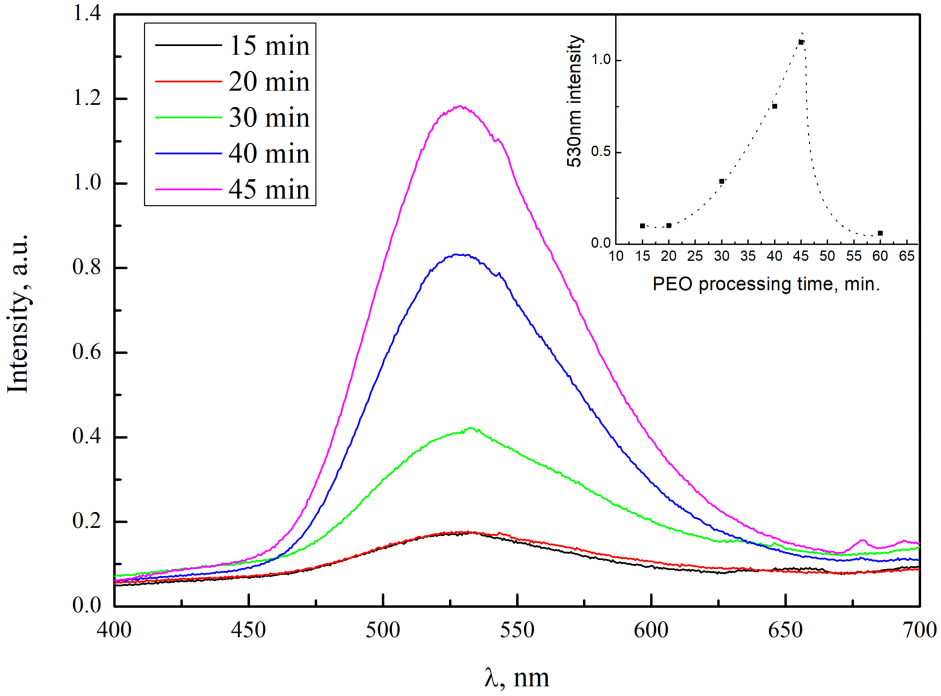

Figure 8. Photoluminescence spectra of samples after different PEO treatment durations. The inset shows the intensity dependence on the PEO processing time.

To perform luminescence decay kinetics measurements, each sample was irradiated with a 405-nm diode laser for 30 s. The kinetics measurements began 3 s after turning off the excitation source. Each measurement was carried out until the kinetics reached a plateau (the dynamic range of the detector is not enough to detect the changes in the intensity), which was around 4 min after ceasing excitation. Despite different initial intensities (shown in the inset of Figure 8), the luminescence decay kinetics characteristics for samples with various PEO treatment times did not vary (Figure 9), as the dual exponent approximation is essentially the same for all the samples. This leads to the conclusion that filling the powder into an aluminum oxide matrix does not disrupt the strontium aluminate powder structure, as expected.

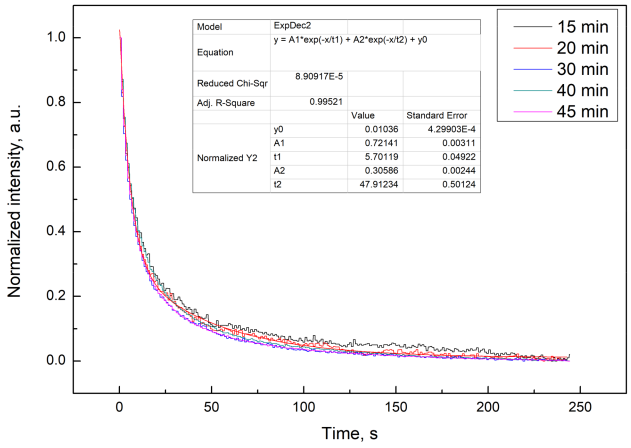

Figure 9. Decay kinetics measured for different samples. Dual exponent approximation results are presented in the inset table.

Although the PEO samples are visible in the dark for a few minutes, the duration of the afterglow is much shorter compared to commercial powder samples. This might be due to some surface effects that need to be studied in more detail.

4. Conclusions

During this study, it was shown that it is possible to produce phosphorescent PEO samples using activated commercial strontium aluminate powder and the pore-filling method. It was found that a longer PEO treatment duration leads to the development of larger and more densely packed pores and cavities, which in turn facilitates the filling process. The particle size of commercial strontium aluminate powder is too large to fit into the cavities of PEO coatings, so the powder needs to be milled to reduce the particle size. Luminescence measurements showed that milling and filling processes do not change the luminescence characteristics of the strontium aluminate powder, although the luminescence intensity is decreased. It was shown that PEO treatment duration influences luminescence intensity, which is directly related to the amount of powder that is incorporated into the coating. Treatment times until 45 min showed increasing luminescence intensity, but longer treatment times decreased luminescence intensity.

This method could prove useful for many practical applications where both surface protection and phosphorescent properties are necessary. Unfortunately, there are some drawbacks to this method. Although the substrate material is well protected from environmental effects, the incorporated powder is still vulnerable and prone to damage if exposed to water for prolonged periods of time. This means that the coatings should be additionally treated with some type of lacquer to reduce the degradation of the phosphorescent coating. Another obstacle that must be addressed in the future is how to ensure a larger amount of particles to incorporate into the coating and achieve more homogenous and denser distribution. Nevertheless, this method is promising and could be used as a substitute to currently used phosphorescent paints.

Author Contributions: Conceptualization, K.S. and D.M.; Data curation, K.A., A.Z., I.B. and K.L.; Formal analysis, I.B., K.L. and V.V.; Funding acquisition, K.S.; Investigation, A.Z., K.S. and D.M.; Methodology, K.A., A.Z., I.B., K.L. and V.V.; Project administration, K.S.; Resources, I.B. and K.S.; Software, A.Z.; Supervision, K.S.; Validation, K.A.; Visualization, K.A.; Writing – original draft, K.A. and K.S.; Writing – review & editing, K.A., K.S. and D.M.

Funding: This research project was supported financially by ERDF Project No: Nr.1.1.1.1/16/A/182.

Conflicts of Interest: The authors declare no conflict of interest.

References

1. Shionoya, S.; Yen, W.M. *Phosphor Handbook*, 1st ed.; CRC Press LLC: Boca Raton, FL, USA, 1999; pp. 655–658.
2. Lange, H. Luminescent europium activated strontium aluminate. US Patent US3294699A, 27 December 1966.
3. Matsuzawa, T. A New Long Phosphorescent Phosphor with High Brightness, $SrAl_2O_4$:Eu^{2+},Dy^{3+}. *J. Electrochem. Soc.* **1996**, *143*, 2670. [CrossRef]
4. Haranath, D.; Shanker, V.; Chander, H.; Sharma, P. Studies on the decay characteristics of strontium aluminate phosphor on thermal treatment. *Mater. Chem. Phys.* **2003**, *78*, 6–10. [CrossRef]
5. Lv, H.; Pan, Z.; Wang, Y. Synthesis and mechanoluminescent property of (Eu2+, Dy3+)-co-doped strontium aluminate phosphor by soft mechanochemistry-assisted solid-state method. *J. Lumin.* **2019**, *209*, 129–140. [CrossRef]
6. Peng, T.; Yang, H.; Pu, X.; Hu, B.; Jiang, Z.; Yan, C. Combustion synthesis and photoluminescence of SrAl2O4:Eu,Dy phosphor nanoparticles. *Mater. Lett.* **2004**, *58*, 352–356. [CrossRef]
7. Peng, T.; Huajun, L.; Yang, H.; Yan, C. Synthesis of SrAl2O4:Eu, Dy phosphor nanometer powders by sol–gel processes and its optical properties. *Mater. Chem. Phys.* **2004**, *85*, 68–72. [CrossRef]
8. Chang, C.; Yuan, Z.; Mao, D. Eu2+ activated long persistent strontium aluminate nano scaled phosphor prepared by precipitation method. *J. Alloys Compd.* **2006**, *415*, 220–224. [CrossRef]
9. Botterman, J.; Smet, P.F. Persistent phosphor SrAl2O4:Eu,Dy in outdoor conditions: saved by the trap distribution. *Opt. Express* **2015**, *23*, 868–881. [CrossRef]

10. Lu, X.; Blawert, C.; Kainer, K.U.; Zhang, T.; Wang, F.; Zheludkevich, M.L. Influence of particle additions on corrosion and wear resistance of plasma electrolytic oxidation coatings on Mg alloy. *Surf. Coatings Technol.* **2018**, *352*, 1–14. [CrossRef]
11. Sieber, M.; Simchen, F.; Morgenstern, R.; Scharf, I.; Lampke, T. Plasma Electrolytic Oxidation of High-Strength Aluminium Alloys—Substrate Effect on Wear and Corrosion Performance. *Metals (Basel).* **2018**, *8*, 356. [CrossRef]
12. Rokosz, K.; Hryniewicz, T.; Gaiaschi, S.; Chapon, P.; Raaen, S.; Matýsek, D.; Dudek, Ł.; Pietrzak, K. Novel Porous Phosphorus–Calcium–Magnesium Coatings on Titanium with Copper or Zinc Obtained by DC Plasma Electrolytic Oxidation: Fabrication and Characterization. *Materials (Basel)* **2018**, *11*, 1680. [CrossRef]
13. Apelfeld, A.V.; Ashmarin, A.A.; Borisov, A.M.; Vinogradov, A.V.; Savushkina, S.V.; Shmytkova, E.A. Formation of zirconia tetragonal phase by plasma electrolytic oxidation of zirconium alloy in electrolyte comprising additives of yttria nanopowder. *Surf. Coatings Technol.* **2017**, *328*, 513–517. [CrossRef]
14. Yerokhin, A.L.; Nie, X.; Leyland, A.; Matthews, A.; Dowey, S.J. Plasma electrolysis for surface engineering. *Surf. Coatings Technol.* **1999**, *122*, 73–93. [CrossRef]
15. Yerokhin, A.L.; Snizhko, L.O.; Gurevina, N.L.; Leyland, A.; Pilkington, A.; Matthews, A. Discharge characterization in plasma electrolytic oxidation of aluminium. *J. Phys. D. Appl. Phys.* **2003**, *36*, 2110–2120. [CrossRef]
16. Rahmati, M.; Raeissi, K.; Toroghinejad, M.R.; Hakimizad, A.; Santamaria, M. Effect of Pulse Current Mode on Microstructure, Composition and Corrosion Performance of the Coatings Produced by Plasma Electrolytic Oxidation on AZ31 Mg Alloy. *Coatings* **2019**, *9*, 688. [CrossRef]
17. Joost, W.J.; Krajewksi, P.E. Towards magnesium alloys for high-volume automotive applications. *Scr. Mater.* **2017**, *128*, 107–112. [CrossRef]
18. Huda, Z.; Taib, N.I.; Zaharinie, T. Characterization of 2024-T3: An aerospace aluminum alloy. *Mater. Chem. Phys.* **2009**, *113*, 515–517. [CrossRef]
19. Bouali, A.C.; Straumal, E.A.; Serdechnova, M.; Wieland, D.C.F.; Starykevich, M.; Blawert, C.; Hammel, J.U.; Lermontov, S.A.; Ferreira, M.G.S.; Zheludkevich, M.L. Layered double hydroxide based active corrosion protective sealing of plasma electrolytic oxidation/sol-gel composite coating on AA2024. *Appl. Surf. Sci.* **2019**, *494*, 829–840. [CrossRef]
20. Lu, X.; Chen, Y.; Blawert, C.; Li, Y.; Zhang, T.; Wang, F.; Kainer, K.U.; Zheludkevich, M. Influence of SiO2 Particles on the Corrosion and Wear Resistance of Plasma Electrolytic Oxidation-Coated AM50 Mg Alloy. *Coatings* **2018**, *8*, 306. [CrossRef]
21. Akatsu, T.; Yamada, Y.; Hoshikawa, Y.; Onoki, T.; Shinoda, Y.; Wakai, F. Multifunctional porous titanium oxide coating with apatite forming ability and photocatalytic activity on a titanium substrate formed by plasma electrolytic oxidation. *Mater. Sci. Eng. C* **2013**, *33*, 4871–4875. [CrossRef]
22. Grigorjeva, L.; Millers, D.; Smits, K.; Zolotarjovs, A. Gas sensitive luminescence of ZnO coatings obtained by plazma electrolytic oxidation. *Sensors Actuators A Phys.* **2015**, *234*, 290–293. [CrossRef]
23. Zolotarjovs, A.; Smits, K.; Laganovska, K.; Bite, I.; Grigorjeva, L.; Auzins, K.; Millers, D.; Skuja, L. Thermostimulated luminescence of plasma electrolytic oxidation coatings on 6082 aluminium surface. *Radiat. Meas.* **2019**, *124*, 29–34. [CrossRef]
24. Park, S.Y.; Jo, C.I.; Choe, H.-C.; Brantley, W.A. Hydroxyapatite deposition on micropore-formed Ti-Ta-Nb alloys by plasma electrolytic oxidation for dental applications. *Surf. Coat. Technol.* **2016**, *294*, 15–20. [CrossRef]
25. Kang, J.-I.; Son, M.-K.; Choe, H.-C.; Brantley, W.A. Bone-like apatite formation on manganese-hydroxyapatite coating formed on Ti-6Al-4V alloy by plasma electrolytic oxidation. *Thin Solid Films* **2016**, *620*, 126–131. [CrossRef]
26. Smits, K.; Millers, D.; Zolotarjovs, A.; Drunka, R.; Vanks, M. Luminescence of Eu ion in alumina prepared by plasma electrolytic oxidation. *Appl. Surf. Sci.* **2015**, *337*, 166–171. [CrossRef]
27. Stojadinović, S.; Tadić, N.; Vasilić, R. Photoluminescence of Sm2+/Sm3+ doped Al2O3 coatings formed by plasma electrolytic oxidation of aluminum. *J. Lumin.* **2017**, *192*, 110–116. [CrossRef]
28. Bite, I.; Krieke, G.; Zolotarjovs, A.; Laganovksa, K.; Liepina, V.; Smits, K.; Auzins, K.; Grigorjeva, L.; Millers, D.; Skuja, L. Novel method of phosphorescent strontium aluminate coating preparation on aluminum. *Mater. Des.* **2018**, *160*, 794–802. [CrossRef]

29. Martin, J.; Leone, P.; Nominé, A.; Veys-Renaux, D.; Henrion, G.; Belmonte, T. Influence of electrolyte ageing on the Plasma Electrolytic Oxidation of aluminium. *Surf. Coat. Technol.* **2015**, *269*, 36–46. [CrossRef]
30. Liepina, V.; Millers, D.; Smits, K. Tunneling luminescence in long lasting afterglow of SrAl2O4:Eu,Dy. *J. Lumin.* **2017**, *185*, 151–154. [CrossRef]
31. Aitasalo, T.; Dereń, P.; Hölsä, J.; Jungner, H.; Krupa, J.-C.; Lastusaari, M.; Legendziewicz, J.; Niittykoski, J.; Stręk, W. Persistent luminescence phenomena in materials doped with rare earth ions. *J. Solid State Chem.* **2003**, *171*, 114–122. [CrossRef]

Institute of Solid State Physics, University of Latvia as the Center of Excellence has received funding from the European Union's Horizon 2020 Framework Programme H2020-WIDESPREAD-01-2016-2017-TeamingPhase2 under grant agreement No. 739508, project CAMART²